Determination of sea conditions for wave energy conversion by spectral analysis

B. Yagci[1] and P. Wegener[2]

[1]School of Aeronautics and Astronautics,
Purdue University,
W. Lafayette, Indiana, USA
E-mail: baris.yagci@gmail.com

[2]Waveberg Development Ltd.,
New York City, New York, USA
E-mail: pwegener@waveberg.com

Abstract

Conversion of wave motion to electrical energy depends on the instantaneous sea state at a given location, which can change on second, minute and hour timescales. In particular, information about wave groupiness (sets) is important in determining the efficiency of a wave energy converter at a given location. We report the use of a spectral method to analyze buoy time data to determine the sea state and express it as average wave height and period, as well as percentage slack time when the waves are smaller than the converter can use. The proposed method is a sinusoid estimation algorithm based on Capon's maximum likelihood estimate, which converges to the point spectrum of the sinusoids in the wave data. Therefore one can estimate sinusoid frequencies and amplitudes from a signal corrupted by noise. Present method is compared against FFT in frequency domain. The results of these spectral methods are used to obtain statistical characteristics of waves. As a golden standard, the same wave characteristics are also determined using a peak finding algorithm. The statistical wave data is then used to predict the power output of the wave energy converter using a model derived from experimental data. The implications for "harmonic" versus non-harmonic devices are discussed briefly.

Keywords: Non-stationary noise, spectral analysis, wave sets, wave statistics.

1 Introduction

In this paper a stochastic method is used to estimate the dominant frequencies and their amplitudes present in segments of ocean waves. The method is based on Capon-Geronimus algorithm presented in [1–4]. The results used in this note gives an estimate of the frequency spectrum of the data corrupted by noise which converges to the point spectrum as the data set gets larger. In the limit, the amplitude of the spectrum converges to the amplitude of the underlying sinusoids in the corrupted signal. The convergence result of the method makes it a practical tool for distinguishing peaks due to sinusoids in the spectrum from the peaks that may occur due to noise process.

A very common tool used in determining dominant frequencies is Fast Fourier Transform (FFT), which assumes deterministic and periodic signals as input. Since FFT is a well established method used in industry, we compare the results of Capon's method with results of FFT.

In addition to FFT and Capon's methods, a peak finding algorithm is used to gather peak height and frequency information. The peak-finding algorithm is used as a gold standard for comparison because it provides the actual heights and periods of ocean waves. We use the algorithm to find both peaks and troughs, and comparison shows the two distributions to be identical, as expected in deep water. Comparison of both Capon's method and FFT shows these techniques introduce a consistent bias into the estimation of wave statistics, but Capon's method is less biased than FFT.

The aim of the ocean wave analysis in this work is to predict the power output of a wave energy converter. The results of the analysis are used as an input to an experimental power output model of a Waveberg waver energy converter. Data from various sites and different seasons are chosen to predict the power output of the device.

The wave data were obtained from the Coastal Data Information Program (CDIP) website and supplied as a favor from Channel Coastal Observatory (CCO) UK. Both institutions use Datawell Mark II buoys at these locations, with a 1.28 Hz sampling rate. A third set of data set is supplied by Hydraulics & Maritime Research Centre, University College Cork, Ireland, measured by a non-directional Datawell buoy,sampled at 2.56Hz. We use only the vertical (heave) component of the motion as an input.

2 Comparison of Capon's method to FFT

Fast Fourier Transform(FFT) is commonly used to determine the frequency content of a signal. The FFT assumes that the input signal is periodic; Capon's method does not have such a restriction. When the input signal is corrupted by noise, it will no longer be periodic. An outline of Capon's method is given in the Appendix.

Consider a short segment of ocean wave data that encompasses a full period of a single wave, as plotted in Fig. 1. The wave height of this particular wave is 177cm, which corresponds to an amplitude of 88.5cm. The period is 13.3 seconds and the frequency is 0.47rad/s. The spectra of this signal was calculated both with Capon's method and FFT and are shown in Fig. 2-(a) and (b), respectively. In each case the spectrum is normalized with respect to the spectrum of a sine wave sampled with the same sampling rate and duration. No windowing is applied in either case.

In Fig. 2-b, we see that FFT has introduced side lobes, since the input signal is not periodic. The spectrum obtained by Capon's method does not have such artifacts. The number and size of side lobes can be decreased using windowing and other techniques in FFT spectrum calculations, however this would effect the amplitude estimations [5]. Capon's method underestimates the actual amplitude by 3.25%, while FFT underestimates it by 9.04%. The frequency of this single wave is estimated to be 13.83% lower than the actual by Capon's method and 15.36% by FFT. Thus both methods give a reasonable estimate of the underlying sinusoid process when a single wave is presented as input, with the Capon's estimate slightly more accurate and without artifacts.

Longer data segments are used to generate statistical data to compare the methods. Data from a CDIP buoy, January 16, 2007 outside of Humboldt Bay, California is used for this purpose. First, a 1000 second long time signal in segments of 15.625s is fed to each method. This length of time encompasses period of most of the single waves in this example and it is a multiple of the buoy sampling rate. The results are plotted in Fig. 3. The amplitude and frequency information obtained with each method is consistent over the length of the data. Second, for a statistical comparison a 12 hour long data from the same date and buoy are processed with Capon's method and FFT. The results are given in Table 1. Both methods give statistically very similar wave amplitude.

Table 1: Statistical properties of wave amplitude distributions obtained using Capon's method and FFT. CDIP, Humboldt Bay(128) buoy, January 16, 2007 data.

Method	Capon	FFT
Mean, cm	39.29	38.46
Median, cm	36.18	35.39
Standard Deviation, cm	18.33	18.69
Skewness	0.93	0.98

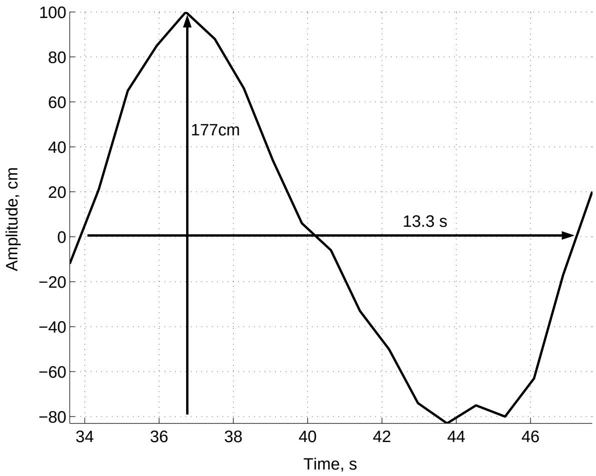

Figure 1: CDIP, Humboldt Bay(128) buoy, January 16, 2007 partial time data. Amplitude of the wave is 88.5cm and the frequency is 0.47 rad/s.

3 Slack time estimation

The ocean waves are very rich in frequency content. Moreover, waves come in sets of higher heights, followed by periods with little or no wave activity. The use of significant wave height, H_S, as a summary statistic obscures the groupiness of waves, as H_S is defined as the average of the highest 1/3 of the waves. Any spectral method applied over a long period of time will superimpose a simplified distribution of the ocean wave spectrum. Here we are most interested in the wave heights at a given time and the time between wave groups. To get this information from the spectrum, Capon's Theorem 6.1 is applied on a series of segments of time data much shorter than the sets. In this way, the time variation of the spectra is preserved..

A gold standard for determining the height and time lapse of each wave is visual inspection of the time trace. Here we use a peak detection algorithm to find peak heights in amplitude and when they occur; the time between successive peaks in a given segment of wave data is determined by subtraction. The peak detection algorithm used in this paper is written by Tom O'Haver [6]. The method utilizes the smoothed third derivative of the signal to find the peaks. It is easier to apply than FFT or Capon's method for wave data where the frequency of the waves vary over a wide range. Although the algorithm is very efficient finding peaks, it requires tuning several parameters to the wave record in question and is hard to implement for automated analysis.

Figure 4 shows the spectrum, peak time differences, and between-wave time data for 1000 seconds (16.7 minutes) on January 16, 2007 outside of Humboldt Bay, California. In Fig. 4-a, the spectrum consists of 64 time segments of 15.625 seconds length, each containing 20 height samples (1.28 Hz sampling rate). Spectrum estimate from each time segment is plotted with respect to the time the segment started. The blue color shows lower amplitudes and the highest waves are represented in red color. Figure 4-b is a plot of time differences be-

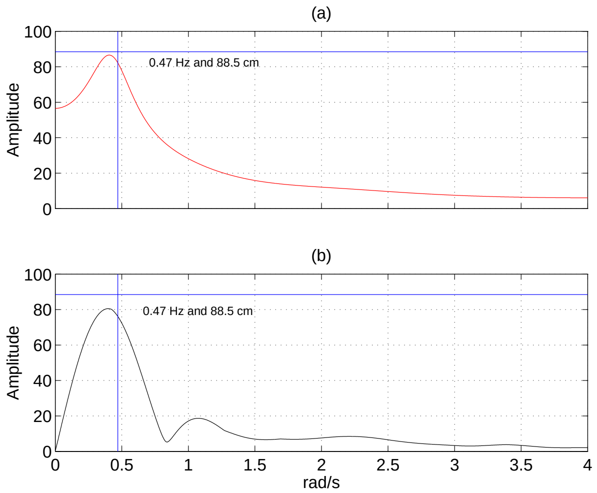

Figure 2: CDIP, Humboldt Bay(128) buoy, January 16, 2007. Spectrum of partial time data given in Fig. 1. Plot (a) is the result of application of Theorem 6.1; the peak occurs at 0.405 rad/s and 86.6 cm amplitude. Plot (b) is result of application of FFT; the peak occurs at 0.3978 rad/s and 80.5 cm. The crosshair indicates actual wave data.

tween the consecutive peaks detected by the peak finding algorithm. The time trace is given in Fig. 4-c, where peaks detected by the peak finding program are marked on the plot with a red cross. The circles represent the amplitude estimate from Capon's method for that time segment. The agreement of the results is also visible through inspection of Fig. 5. Both results agree very well and follow the actual wave peaks. One advantage of using the spectral method over the peak finding algorithm in this application is that spectral method does not require fine adjustment of the parameters to detect wave height. Even though it is very effective, the peak finding algorithm needs adjustment of number of point to apply smoothing to, and the number of points around the top part of the peak. These parameters have an effect on the number of peaks detected.

The threshold amplitude for sea conditions to be considered flat would be the wave height below which a wave energy converter cannot produce power. Consider the wave height power curve given Fig. 8, at wave height of 0.36 meters the particular wave energy converter stops providing electrical energy. For this device and the sea conditions considerd in this section, the dead time is 148.55 seconds over 1000 seconds using the spectral amplitude estimation. Over the same time period, using the peaks determined with the peak finding algorithm the dead time is calculated to be 150 seconds.

Both Capon's method and the peak finding algorithm were run on 12 hours data from the Humboldt Bay buoy, January 16th. The wave height histograms are given in Fig. 6. The wave height frequencies are normalized with respect to the highest bin in each histogram. The statistical properties of two distributions are given in Table 2 and are practically identical.

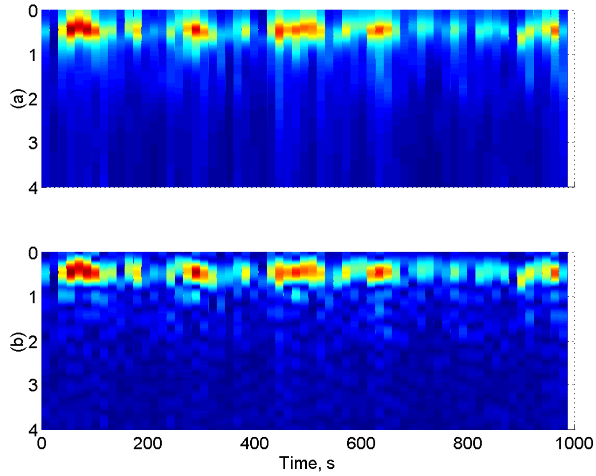

Figure 3: CDIP, Humboldt Bay(128) buoy, January 16, 2007. Spectrum of time data segments of length 15.625s computed by (a) Capon's method, rad/s (b) FFT, rad/s.

Table 2: Statistical properties of wave amplitude distributions obtained using time domain and spectral methods. CDIP, Humboldt Bay(128) buoy, January 16, 2007 data. Compare with Table 1

Method	Peak Finding	Capon
Mean, cm	40.19	39.29
Median, cm	37.00	36.18
Standard Deviation, cm	18.42	18.33
Skewness	0.8	0.93

3.1 Wave amplitude vs. wave height

The result of Capon's method gives the amplitude of the waves, i.e. crest height above the flat ocean surface, or conversely, the depth of the trough. Wave height from trough to crest is the common measure in ocean wave analysis, since in storms and shallow water the form is not a monochromatic sinusoid. The spectral methods used in this study look for the amplitudes sinusoids in the ocean waves, so we assume that wave amplitude is half of wave height when these methods are used. On the other hand, the peak finding algorithm only detects the peaks in time domain and does not assume that there are underlying sinusoids in the ocean waves. This algorithm detects either crests or troughs. Fig. 7,-a shows the crest amplitude histogram and Fig 6 - b shows the trough amplitude histogram from the same 12 hour period. The bottom histogram is an overlap of the previous two. The histograms are virtually identical in shape, as are their statistical properties shown in Table 3. The assumption of wave height is twice the amplitude is valid in this everyday ocean state in deep water.

3.2 Slack time estimation in different geographical areas

Four buoy sites are used in this paper for slack time analysis. The location information of the buoys are given in Table 4. The sites are chosen from different parts of the world to exercise the algorithm with various wave

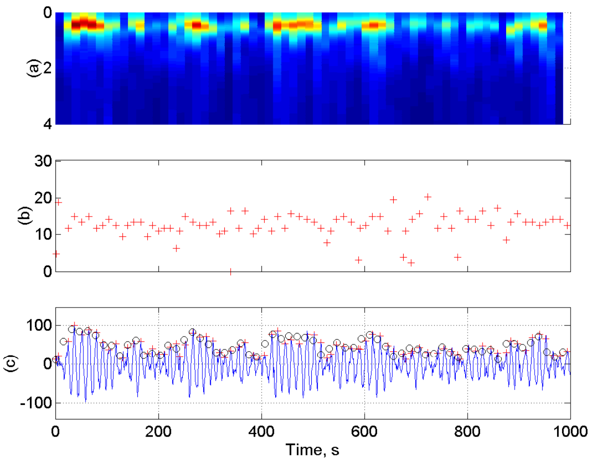

Figure 4: CDIP, Humboldt Bay(128) buoy, January 16, 2007. The vertical axis of the plots are; (a) Frequency, rad/s, (b) Time between peaks, s, (c) Wave height, cm. Plot (a) is the shifted spectrum of the time data, (b) is the time difference between the peaks determined using the peak finding algorithm, (c) is the time data with peaks marked with red crosses found using the peak finding algorithm and circles using Theorem 6.1

Table 3: Statistical properties of wave crest and trough distributions obtained using peak finding algorithm. CDIP, Humboldt Bay(128) buoy, January 16, 2007 data

Method	Crest	Trough
Mean, cm	40.19	40.30
Median, cm	37	38
Standard Deviation, cm	18.42	18.17
Skewness,	0.8	0.76

regimes. Along the same lines, data from summer and winter seasons in certain sites are evaluated. Two of these sites are in Pacific Ocean; Humboldt Bay, South Spit, California (A, B) and Ipan, Guam (C,D). The letters in the parenthesis indicate the name of the buoy in Table 4. These sites are operated by Coastal Data Information Program (CDIP). Third site is in Perranporth, Cornwall, UK on the Atlantic Ocean side of the British Isles. This site is operated by Channel Coastal Observatory (CCO). The fourth site is off the coast of Western Ireland, this buoy data is supplied by Hydraulics & Maritime Research Centre, University College Cork.

Predicted power output and slack time at various locations are summarized in Table 5.

4 Experimental power output model

The Waveberg is a floating attenuator that works in heave. The power output is strictly a function of wave height, similar to point absorbers [7]. However, unlike a point-absorber, the Waveberg has an equal response to wave heights across a broad range of the frequency spectrum; this result is not intuitively obvious and further investigations are underway to explore this phenomenon. Nonetheless, in regular tank waves, the following linear relation between the power output and mean wave height

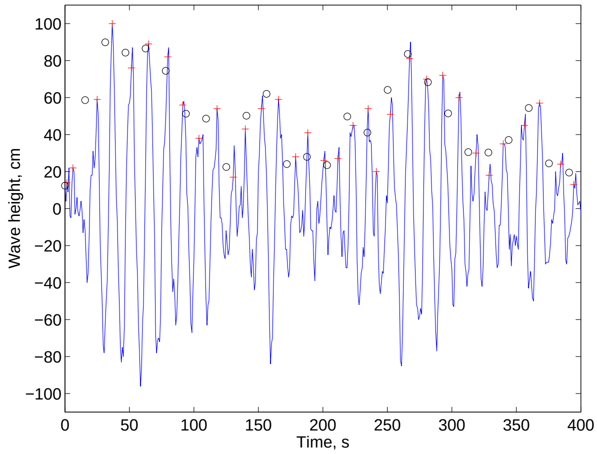

Figure 5: CDIP, Humboldt Bay(128) buoy, January 16, 2007. Time data of the ocean wave. The crosses indicate the peaks found by the peak finding algorithm and the circles indicate the estimated wave heights in a given 15.625 second time segment.

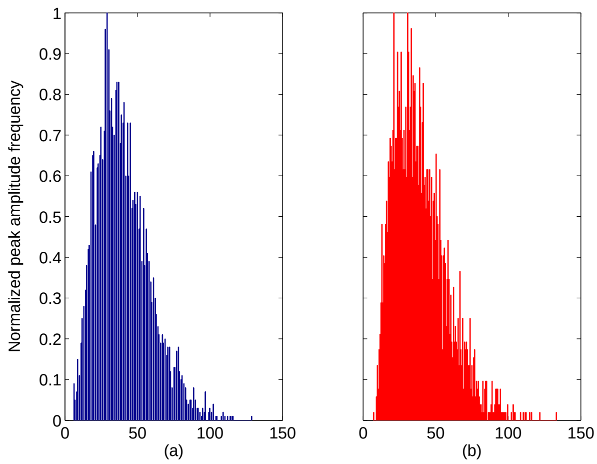

Figure 6: CDIP, Humboldt Bay(128) buoy, January 16, 2007. Histograms of the normalized peak amplitudes using, a) Peak finding algorithm, b) Capon's method. Horizontal axis in cm.

holds true with a determination coefficient of R^2~0.9.

$$P_{out} = F_{con} \times (H_m - H_{min}) \tag{1}$$

This relation works for wavelengths from $0.43 - 1.7$ times the Waveberg length. Here F_{con} is the conversion factor or slope of the line, H_m is the mean wave height, and H_{min} is the horizontal axis intercept, the minimum wave size needed for power conversion. In the case of real-world waves, we set H_{min} as the cut-off size to determine the proportion of slack time (τ_{slack}), taking this in to account, the power - wave relation can be expressed as:

$$P_{out} = (1 - \tau_{slack}) \times F_{con} \times (H_m - H_{min}) \tag{2}$$

Figure 8 shows experimental data illustrating this relation. The model shown here is 1.63 meters long, or 1:40 of a typical full-size Waveberg. The model has losses from the pumps which manifests itself as a shift of the power curve to the right on the horizontal axis. In

Table 4: Information about the data used for the analysis

Name	Location (Approximate)	Date	Water dept (m)	Sampling Rate (Hz)
A	40° 45'N 124° 18' W	January 16, 2007	40	1.28
B	40° 45'N 124° 18' W	July 01, 2007	40	1.28
C	13° 21'N 144° 47' E	January 01, 2007	200	1.28
D	13° 21'N 144° 47' E	July 01, 2007	200	1.28
E	50° 21'N 5° 10' W	December 21, 2007	10	1.28
F	50° 21'N 5° 10' W	June 20, 2008	10	1.28
G	52° 39'N 9° 47' W	February 11, 2005	55	2.56

Table 5: Wave statistics and predicted Waveberg power output

Name	H_m (cm)	P_{out} (KW)	Slack time %	Data length (hr)
A	78.58	90.1	15	12
B	58.45	48.16	12	12
C	154.53	246.70	$<$1	12
D	50.15	30.35	15	12
E	103.07	155.53	$<$1	12
F	146.58	253.14	$<$1	12
G	302.95	572.68	$<$1	1/3

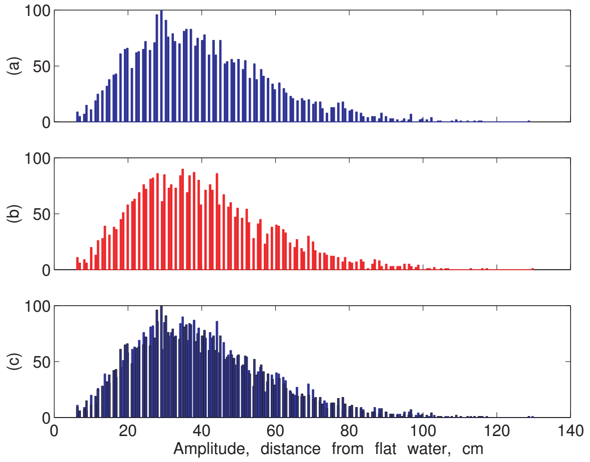

Figure 7: CDIP, Humboldt Bay(128) buoy, January 16, 2007. Histograms of the amplitude of ocean waves as measured from the flat water surface. (a) Frequency of the peaks (crests). (b) Frequency of the troughs. (c) Frequency, histograms in (a) and (b) overlapped.

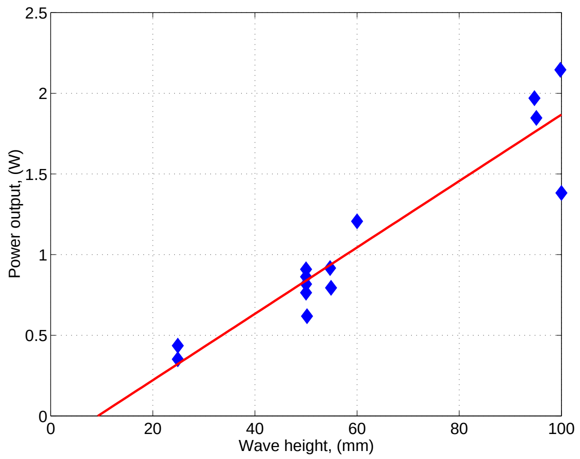

Figure 8: Experimental power output data for scale model of Waveberg. The experimental data is indicated with diamond points, the line is a third order polynomial fit.

the full scale case, minimum wave height $H_{min} = 0.9mm$ would translate into $H_{min} = 0.36m$. Power conversion factor when scaled is 214.52 KW per meter wave height.

Thus the key determinants of wave power available at a site are average wave height H_m, the period of the swell wave T_P, and the proportion of slack time. Capon's method determines all three parameters from the buoy data and can be automated to analyze archived data. The method can provide far more relevant information about the sea states at a proposed wave energy conversion site than the traditional H_S and T_z. Previously, buoy data has been analyzed primarily for safety considerations and ship navigation, and the traditional parameters have been adequate for that purpose. Now we need to generate a new analysis for wave energy conversion, and Capon's method appears ideal for this purpose.

As an example consider the CDIP, Humboldt Bay(128) buoy. The mean wave height for the 12 hours time period considered in the previous section H_m = 0.78m as estimated by Capon's method. Using Fig. 8 the power output of a Waveberg at this sea state would be 90.1 KW.

5 Conclusions

Capon's method detects peaks very effectively without need of fine parameter adjustment or windowing. The amplitude estimates obtained with this method are used to obtain statistical characteristics of ocean waves at a given location. This information is crucial in determining the operation location as well as sizing the energy converter.

The strength of Capon's method is convergence of estimated spectrum to point spectrum at the sinusoid frequencies, while approaching zero everywhere else. This property is used to disregard peaks that may appear as a result of noise process when a small number of samples is used. The weakness of the method is the higher computational cost than FFT. However, properly automated, Capon's method can analyze large samples of archived data in reasonable time periods for assessment of energy conversion.

6 Appendix

6.1 Spectral frequency and amplitude estimation

Let $y(n)$ be the discrete measurements of vertical surface displacement of the ocean expressed as;

$$y(n) = \xi(n) + \zeta(n). \tag{3}$$

Here $\zeta(n)$ is a non-stationary noise process. The first part, $\xi(n)$ is the stationary part of the ocean waves in consideration [8] and it is assumed to be composed of sinusoids;

$$\xi(n) = \sum_{k=1}^{\nu} a_k e^{\imath(\omega_k n + \phi_k)} \tag{4}$$

where $\{\omega_k\}_1^\nu$ are distinct angular frequencies, $\{a_k\}_1^\nu$ are the corresponding amplitudes and $\{\phi_k\}_1^\nu$ are independent random variables uniformly distributed over the interval $[0, 2\pi]$.

The autocorrelation function $R_y(n_1, n_2)$ of $y(n)$ is given by,

$$R_y(n_1, n_2) = E(y(n_1)y(n_2)). \tag{5}$$

Here $E(.)$ is the expectation. When $R_y(n_1, n_2)$ can be expressed in terms of the difference $n_1 - n_2$ and $Ey(n)$ is constant, then y(t) is wide sense stationary. Ocean waves are partly produced by action of winds over the water surface. These effects are intermittent in time and the autocorrelation function of $y(n)$ can not be expressed in terms of $n_1 - n_2$. The mean of $y(n)$ obtained from different segments of the data will attain different values. In this case, ocean waves are termed to be non-stationary.

The sinusoid estimation algorithm presented here uses a portion of the data $\{y(k)\}_{k=-\infty}^{k=n}$. Consider the following random process defined by,

$$x(n) = \sum_{k=-\infty}^{n} A_m^{n-k} B_m y(k). \tag{6}$$

Here A_m is a stable matrix on $\mathbb{C}^m$ with all its eigenvalues in the unit circle and the pair $\{A_m, B_m\}$ is controllable. The matrix B is defined from $\mathbb{C}$ into $\mathbb{C}^m$. Let T_{yn} be the covariance matrix for y defined by,

$$T_{yn} = \begin{bmatrix} R_y(n,n) & R_y(n,n-1) & R_y(n,n-2) & \cdots \\ R_y(n-1,n) & R_y(n-1,n-1) & R_y(n-1,n-2) & \cdots \\ R_y(n-2,n) & R_y(n-2,n-1) & R_y(n-2,n-2) & \cdots \\ \vdots & \vdots & \vdots & \ddots \end{bmatrix}. \tag{7}$$

Note that $T_{yn} = T_\xi + T_{\zeta n}$. The only assumption on the noise process $\zeta(n)$ is that its covariance matrix $T_{\zeta n}$ is bounded. Equivalently, $0 < T_{\zeta n} \leq I\beta$ for some positive β.

The controllability matrix W_m for the pair $\{A_m, B_m\}$ is given by,

$$W_m = \begin{bmatrix} B_m & A_m B_m & A_m^2 B_m & \cdots \end{bmatrix} : \ell_+^2 \to \mathbb{C}^m. \tag{8}$$

Using the definition of $x(n)$, the covariance matrix of $x(n)$ can be expressed as;

$$\begin{aligned} Tx(n)x(n)^* &= \Lambda_m \\ &= W_m T_{yn} W_m^*. \end{aligned} \tag{9}$$

The relation between the present and classical sinusoid algorithm can be seen easily if the pair $\{A_m, B_m\}$ is chosen as such,

$$A_m = \begin{bmatrix} 0 & 1 & 0 & \cdots & 0 \\ 0 & 0 & 1 & \cdots & 0 \\ 0 & 0 & 0 & \cdots & 0 \\ \vdots & \vdots & \ddots & \vdots & \vdots \\ 0 & 0 & \cdots & 0 & 1 \\ 0 & 0 & \cdots & 0 & 0 \end{bmatrix} \text{ on } \mathbb{C}^m \quad \text{and} \quad B_m = \begin{bmatrix} 1 \\ 0 \\ 0 \\ \vdots \\ 0 \end{bmatrix} : \mathbb{C} \to \mathbb{C}^m. \tag{10}$$

The following theorem summarizes the sinusoid estimation algorithm.

Theorem 6.1 *Let y(n) be the random process determined by* $y(n) = \xi(n) + \zeta(n)$ *where* $\xi(n)$ *is the sinusoid process given by (4) and* $\zeta(n)$ *is a random process such that* $0 < T_{\zeta n} \leq I\beta$ *for all integers n. Let* $\Lambda_{m,n} = W_m T_{yn} W_m$ *where* W_m *is the controllability matrix formed by the pair* $\{A_m, B_m\}$ *. Consider the optimization problem,*

$$\mu_m(\lambda) = \inf\{(T_{yn} W_m x, W_m x) : C_m(I - \lambda A_m)^{-1} x = 1\}. \tag{11}$$

Then,

$$\begin{aligned} \lim_{m\to\infty} \mu_m(e^{\imath\omega}) &\leq |a_j|^2 \quad \text{if } \omega = \omega_j \text{ for all } j = 1, 2, \cdots, \nu \\ &= 0 \quad \text{if } \omega \neq \omega_j. \end{aligned} \tag{12}$$

This result shows that the estimate of the spectrum μ_m converges to the point spectrum of the sinusoid process at the sinusoid frequencies. This property is useful in distinguishing peaks due to sinusoids from the peaks due to the noise process. If the estimate of the spectrum is calculated for integers $0 < m_1 < m_2$ then any peak that may appear in $\mu_{m1}(e^{\imath\omega})$ wouldn't appear in $\mu_{m2}(e^{\imath\omega})$, if it is due to a noise process. Moreover, one would observe that at a sinusoid frequency ω_k the spectrum estimate converges to the sinusoid amplitude a_k and zero everywhere else.

The covariance matrix T_{yn} can only be approximated numerically given an experimental signal. To remove the artifacts of this calculation the, estimated spectra are normalized with respect to a peak obtained from a unit amplitude sine wave with 15.625 seconds period. The sine wave is also sampled at 1.28 Hz as the ocean waves used in this study.

Acknowledgements

The authors thank Dr. Travis Mason of CCO for the Perranporth Data and Sean Barrett of Hydraulics & Maritime Research Centre, University College Cork for the Irish data.

7 References

References

[1] J. Capon. High-resolution frequency-wave number spectrum analysis. In *Proc. IEEE*, volume 57, pages 1408–1418.

[2] T. T. Georgiou. Spectral estimation via selective harmonic amplification. *IEEE Trans. Automat. Contr.*, 46:29–42.

[3] C. Foias and A. E. Frazho. A geometric approach to the maximum likelihood spectral estimator for sinusoids in noise. *IEEE Transactions on Information Theory*, 34:10661070, 1988.

[4] S. L. Marple. *Digital Spectral Analysis with Applications*. Prentice-Hall, Englewood Cliffs,, 1987.

[5] R. C. Wu and T. P. Tsao. Theorem and application of adjustable spectrum. *IEEE Transactions on Power Delivery*, 18(2):372–376.

[6] T. O'Haver. *Peak finding and measurement (version 1.6)*. http://www.mathworks.com/matlabcentral /fileexchange/11755, July 2006.

[7] K. Nielsen and C. Plum. Point absorber numerical and experimental results. In *Proceedings Fourth European Wave Power Conference, Aalborg, Denmark*, 2000.

[8] G. J. Komen et al. *Dynamics and Modelling of Ocean Waves*. Cambridge University Press, 1994.